Available online at www.sciencedirect.com
SCIENCE DIRECT®
Journal of Molecular Catalysis A: Chemical 235 (2005) 271–284
JOURNAL OF MOLECULAR CATALYSIS A: CHEMICAL
www.elsevier.com/locate/molcata

Synthesis and characterization of new chiral octadentate nitrogen ligands and related copper(II) complexes as catalysts for stereoselective oxidation of catechols

Michele Gullotti [a,*], Laura Santagostini [a], Roberto Pagliarin [b], Alessandro Granata [c], Luigi Casella [c]

[a] *Dipartimento di Chimica Inorganica, Metallorganica e Analitica, Università di Milano, Istituto ISTM-CNR, Via G. Venezian, 21, 20133 Milano, Italy*
[b] *Dipartimento di Chimica Organica e Industriale, Università di Milano, Via G. Venezian 21, 20133 Milano, Italy*
[c] *Dipartimento di Chimica Generale, Università di Pavia, Via Taramelli 12, 27100 Pavia, Italy*

Received 11 January 2005; received in revised form 21 March 2005; accepted 23 March 2005
Available online 12 May 2005

Abstract

Three new octadentate ligands, namely (*R*)-*N*,*N*′-dimethyl-*N*,*N*′-bis{3-[bis(1-methyl-2-imidazolylmethyl)]aminopropyl}-1,1′-binaphthyl-2,2′-diamine, (*R*)-DABN-3Im$_4$, (*R*)-*N*,*N*′-dimethyl-*N*,*N*′-bis{4-[bis(1-methyl-2-benzimidazolylmethyl)]aminobutyl}-1,1′-binaphthyl-2,2′-dia-mine, (*R*)-DABN-4Bz$_4$, and (*S*)-*N*2,*N*6-dimethyl-*N*2,*N*6-bis{2′-[bis(1-methyl-2-benzimidazolylmethyl)]aminomethyl}benzyl-2,6-dia-mino-1-exanol acetate, L-Lys-4Bz$_4$, were employed for the synthesis of dinuclear and trinuclear copper(II) complexes. The ligands contain two side arms of different nature and length which carry tridentate aminobis(benzimidazole) or aminobis(imidazole) residues as metal binding sites (A sites) connected to a central (*R*)-1,1′-binaphthyl-2,2′-diamine or L-lysine residue which can bind a third metal ion (B site). The chiroptical properties of the ligands and the complexes have been described. The complexes were tested as catalysts in the oxidation of 3,5-di-*tert*-butylcatechol, L-, D-Dopa and L-, D-Dopa methyl esters by dioxygen to give the corresponding quinones. The catalytic efficiency is moderate, but the complexes exhibit significant enantio-differentiating ability towards L-, D-Dopa methyl esters, albeit their enantio-differentiating ability towards L-, D-Dopa is lower. The (*R*)-1,1′-binaphthyl-2,2′-diamine spacer in the (*R*)-DABN complexes has much stronger recognition power than the aliphatic L-lysine spacer in the L-Lys complexes. In addition, the highest stereoselectivity in the catalytic oxidation is obtained with the (*R*)-DABN-3Im$_4$ complexes, containing carbon chains of three atoms between the (*R*)-1,1′-binaphthyl-2,2′-diamine groups and the tridentate donor units at the A metal binding sites. In all cases, the preferred enantiomeric substrate has the L configuration, which is dictated by the chirality of the spacer residue.

Keywords: Copper complexes; Chiral complexes; Trinuclear complexes; Catechol oxidase; Stereoselective oxidations

1. Introduction

In biological systems, the oxidation of organic substrates with molecular oxygen is often carried out by multicopper enzymes, which serve as highly efficient oxidation catalysts [1–6]. These enzymes generally contain dinuclear or trinuclear copper clusters. In the first case, two three-coordinated copper centres with histidine ligands are present, as it was initially shown for hemocyanin, the dioxygen carrier protein in arthropods and molluscs [7]; the best known members of this family are tyrosinase, which catalyzes the hydroxylation of phenols (phenolase activity) and the oxidation of catechols to quinones (catecholase activity) [8,9], and catechol oxidase, which only catalyzes the oxidation of catechols to quinines [10–12]. These proteins are classified as Type 3 copper proteins because their dinuclear clusters are strongly antiferromagnetically coupled and therefore EPR silent in

* Corresponding author. Tel.: +39 02 50314379; fax: +39 02 50314405.
E-mail address: michele.gullotti@unimi.it (M. Gullotti).

1381-1169/$ – see front matter © 2005 Elsevier B.V. All rights reserved.
doi:10.1016/j.molcata.2005.03.031

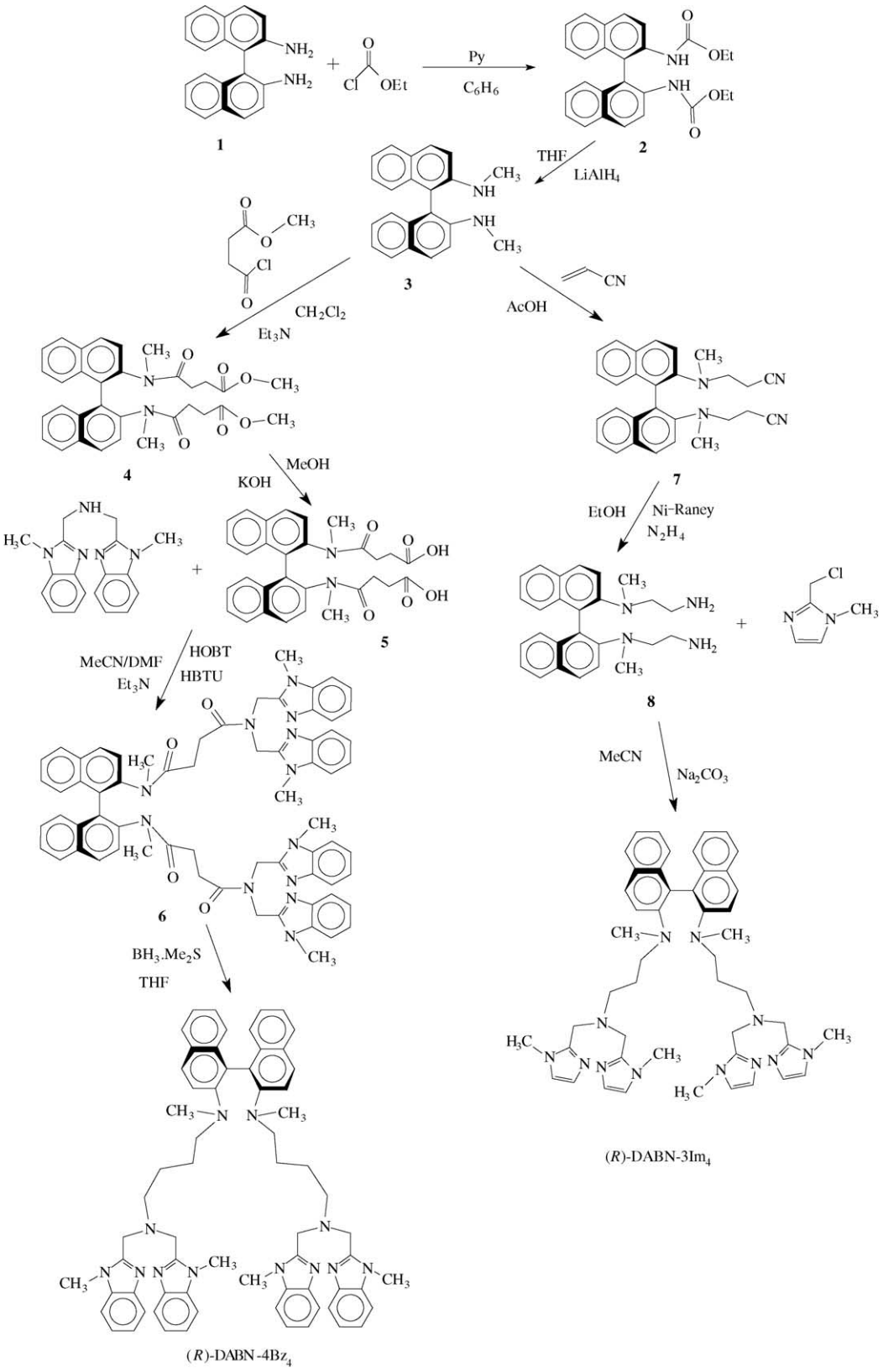

Fig. 1. Synthetic routes for the preparation of the ligands (*R*)-DABN-3Im$_4$ and (*R*)-DABN-4Bz$_4$.

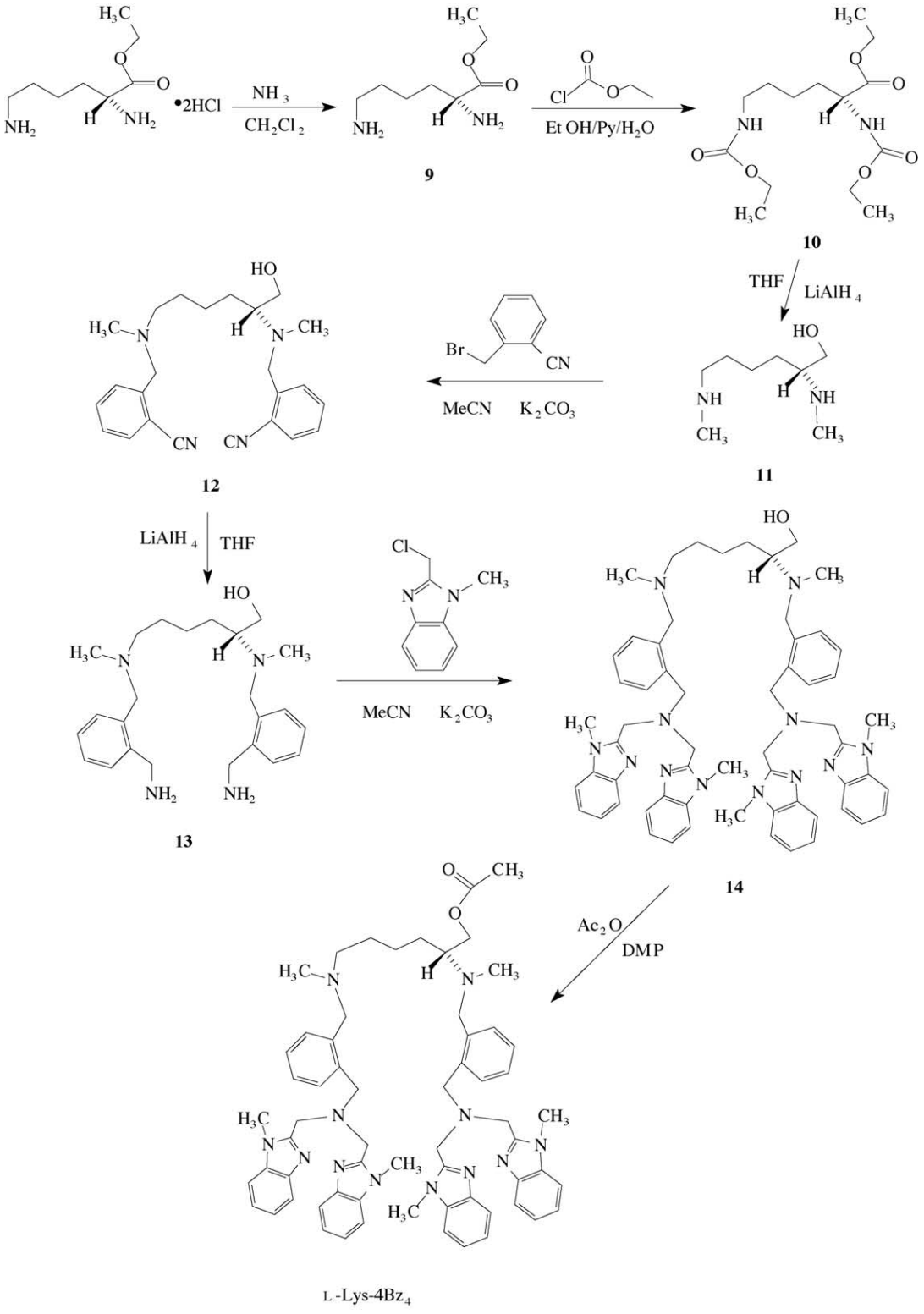

Py = pyridine, DMP = *N,N*-dimethylpyridin-4-amine

Fig. 2. Synthetic route for the preparation of ligand L-Lys-4Bz$_4$.

the oxidized state [5]. Another group of copper proteins such as laccase [13], ascorbate oxidase [14] and ceruloplasmin [15] are active in the oxidation of a variety of substrates and contain trinuclear, Type 2–Type 3 copper clusters. Therefore, the investigation of functional model complexes for metalloenzymes with oxidase or oxygenase activity is potentially useful for the development of new and efficient catalysts for oxidation reactions. Studies from several groups focused on the catechol oxidase activity of copper complexes with different structural features [16–28], and a general result is that dinuclear copper complexes are more efficient than mononuclear complexes. This depends on the fact that two metal centres located in close proximity facilitate the binding of the catechol in a bridging mode and the two-electron transfer step required in the oxidation process. The interest of our group has also focused on dinuclear [24–28], and trinuclear [29–34] copper complexes derived from polydentate nitrogen ligands which show catecholase activity. Some of these compounds contain chiral centres [31–34], and we have demonstrated the possibility to induce stereoselectivity in the catalytic oxidation of L- and D-Dopa derivatives. In the present paper we report the synthesis and chiroptical properties of three new octadentate ligands containing nitrogen donor atoms, namely (*R*)-*N*,*N*′-dimethyl-*N*,*N*′-bis{3-[bis(1-methyl-2-imidazolylmethyl)]aminopropyl}-1,1′-binaphthyl-2,2′-diamine, (*R*)-DABN-3Im$_4$, (*R*)-*N*,*N*′-dimethyl*N*,*N*′-bis{4-[bis(1-methyl-2-benzimidazolylmethyl)]aminobutyl}-1,1′-binaphthyl-2,2′-diamine, (*R*)-DABN-4Bz$_4$, and (*S*)-*N*2,*N*6-dimethyl-*N*2,*N*6-bis{2′-[bis(1-methyl-2-benzimidazolylmethyl)]aminomethyl}benzyl-2,6-diamino-1-exanol acetate, L-Lys-4Bz$_4$, (Figs. 1 and 2). We also report the preparation and preliminary characterization of the dinuclear and trinuclear Cu(II) complexes derived from these ligands, and a comparative kinetic study of their catecholase activity.

The ligand (*R*)-DABN-3Im$_4$ derives from a previously reported ligand [31] (**L**, that in the labeling scheme adopted in this article will be abbreviated as (*R*)-DABN-3Bz$_4$), by replacement of the benzimidazole donors with the biomimetically more significant imidazoles donors. The second ligand, (*R*)-DABN-4Bz$_4$, contains benzimidazole donors but these are connected via binaphthyl rings with side chains containing one more carbon atom than either (*R*)-DABN-3Bz$_4$ or (*R*)-DABN-3Im$_4$. The third ligand has a different design. It contains a chiral L-lysine residue as a central unit, which is much more flexible than the 1,1-binaphthyl moiety previously employed, and this is connected with two arms carrying four benzimidazole donors through a pair of *ortho*-xylyl spacers. We expect that the variations in ligand structure will affect the properties of the resulting copper complexes, in particular with respect to the efficiency and steric course of the catecholase activity. This information is important to build up structure/activity correlations for the emerging family of biomimetic trinuclear copper catalysts.

2. Experimental

2.1. Materials and physical methods

All reagents and solvents were obtained from commercial sources and used without further purification. Acetonitrile (spectral grade) was distilled from potassium permanganate and sodium carbonate; it was then stored over calcium hydride and distilled before use under an inert atmosphere. Tetrahydrofuran was dried by refluxing and distilling from metallic sodium. ^{1}H- and ^{13}C-NMR spectra were recorded with a Bruker AC 300 spectrometer operating at 7.03 T. Elemental analyses were performed at the microanalytical laboratory of the Chemistry Department in Milano. Atomic absorption measurements were performed with a Perkin-Elmer-3100 Spectrometer. MS (ESI) spectra were obtained from a Thermo-Finnigan LCQ Advantage instrument. Optical spectra were obtained with HP 8452A and HP 8453 diode array spectrophotometers equipped with a thermostated cell holder. Circular dichroism spectra were recorded with a Jasco J-500 spectropolarimeter using quartz cells of 0.01 to 2.0 cm path length.

2.2. Syntheses of the ligands

2.2.1. (*R*)-*N*,*N*′-Dimethyl-*N*,*N*′-bis{3-[bis-(1-methyl-2-imidazolylmethyl)]aminopropyl}-1,1′-binaphthyl-2,2′-diamine

(*R*)-DABN-3Im$_4$. (*R*)-*N*,*N*′-Dimethyl-*N*,*N*′-bis[(3-aminopropyl)]-1,1′-binaphthyl-2,2′-diamine (**8**) (240 mg, 0.562 mmol) [32], was dissolved in anhydrous acetonitrile (15 ml). 2-(Chloromethyl)-1-methylimidazole (293.5 mg, 2.25 mmol) [35] and dry sodium carbonate (286 mg, 2.70 mmol) were then added and the mixture was refluxed for 6 h under stirring in a nitrogen atmosphere. The reaction was followed by TLC (silica) using CH_2Cl_2/MeOH/NH_3 (7:2.5:0.5, v:v:v) as eluent. The mixture was cooled to room temperature, the solid material present was filtered off and washed several times with chloroform. The filtrate was dried under vacuum to afford a brown oil in 65% yield. Anal. Calcd. for $C_{48}H_{58}N_{12}$ (803.06): C 71.78; H 7.28; N 20.93. Found: C 71.56, H 7.12, N 20.87. ^{1}H NMR (300 MHz, $CDCl_3$, 25 °C, TMS): δ = 0.74–0.93 (m, 2H, CH_2–N), 1.06–1.27 (m, 2H, CH_2–N), 1.45–1.65 (m, 4H, CH_2–CH_2), 2.35 (s, 6H, CH_3–N–binaphthyl), 3.37–3.30 (t, 4H, CH_2–N–binaphthyl), 3.58 (s, 12H, CH_3–N–imidazole), 3.64 (s, 8H, CH_2–imidazole), 6.65–6.83 (dd, 8H, CH–imidazole), 7.02–7.13 (m, 4H, CH–binaphthyl), 7.20–7.25 (m, 2H, CH–binaphthyl), 7.50–7.64 (m, 6H, CH–binaphthyl). ^{13}C NMR (75.5 MHz, $CDCl_3$, 25 °C, TMS): δ = 23.3, 32.1, 39.3, 51.0, 55.5, 120.5, 122.3, 124.3, 126.5, 128.1, 128.7, 129.0, 130.4, 134.4, 146.2, 150.8. An unambiguous assignment of the ^{1}H and ^{13}C signals was obtained from the combination of ^{1}H–^{13}C HMQC, ^{1}H–^{1}H COSY, DEPT135, and ^{1}H–^{13}C HMBC spectra. MS (ESI): *m*/*z* (%) = 803 (100) $[M + 1]^+$. UV–vis (CH_3CN): λ_{max} (nm)

(ε $(Mm)^{-1}$) = 218 (51,300), 236 (61,000), 256 (56,200), 292 (22,800), 302 sh (18,300), 352 (5800). CD (CH_3CN): λ_{max} (nm) ($\Delta\varepsilon$ $(M\,cm)^{-1}$) = 213 (+66.8), 224 (−43.8), 259 (−29.4), 297 (+8.7), 375 (−3.4).

The ligand (*R*)-*N*,*N*′-dimethyl-*N*,*N*′-bis{4-[bis(1-methyl-2-benzimidazolylmethyl)]aminobutyl}-1,1′-binaphthyl-2,2′-diamine, (*R*)-DABN-4Bz$_4$. was prepared following the synthetic route reported in Fig. 1.

2.2.2. 4-Methoxy-4-oxobutanoic acid

A stirred suspension of dihydrofuran-2,5-dione (8.06 g, 80.58 mmol) and anhydrous methanol (3.13 g, 98.0 mmol) was refluxed for 1 h. After the mixture had become homogeneous, heating was continued for an additional half an hour. After cooling, the excess methanol was removed under vacuum, yielding a white solid of 4-methoxy-4-oxobutanoic acid. Anal. Calcd. for $C_5H_8O_4$ (132.12): C 45.46; H 6.10. Found: C 45.35; H 6.11. ^{1}H NMR (300 MHz, $CDCl_3$, 25 °C, TMS): δ = 2.66 (m, 4H, CH_2), 3.72 (s, 3H, CH_3), 9.85 (s, ^{1}H, COOH).

2.2.3. Methyl-4-chloro-4-oxobutanoate

A stirred suspension of 4-methoxy-4-oxobutanoic acid (1.01 g, 7.7 mmol) and thionyl chloride (6.62 g, 55.6 mmol) was warmed at 40 °C for 3 h. After this time the excess of thionyl chloride was removed, and the residue was distilled under reduced pressure, thus obtaining a pale yellow oil. Anal. Calcd. for $C_5H_7ClO_3$ (150.56): C 39.88; H 4.69. Found: C 40.01; H 4.72. ^{1}H NMR (300 MHz, $CDCl_3$, 25 °C, TMS): δ = 2.67 (t, 2H, CH_2), 3.21 (t, 2H, CH_2), 3.71 (s, 3H, CH_3).

2.2.4. Butanoic acid, 4-{*N*,*N*′-dimethyl-*N*,*N*′-[(1,1′-binaphthalene)-2,2′diyl]-4-oxo, methyl ester (**4**)

(*R*)-*N*,*N*′-Dimethyl-1,1′-binaphthyl-2,2′-diamine (3) [32], (0.49 g, 1.56 mmol) and methyl-4-chloro-4-oxobutanoate (1.63 g, 10.86 mmol) were dissolved in anhydrous dichloromethane (30 ml) under N_2 and the solution was cooled to 0 °C. A solution of Et_3N (0.65 g, 6.43 mmol) in dichloromethane (5 ml) was then added dropwise during 15 min. The mixture was subsequently warmed to room temperature and stirred for 24 h. The reaction, followed by TLC (silica) using light petroleum/ethyl acetate (8:2, v:v) as eluent, was then quenched by the addition of 2N HCl (10 ml); the organic layer was separated and the aqueous layer was extracted with dichloromethane (3 × 30 ml). The organic layers were dried with Na_2SO_4 and the solvent was removed by rotary evaporation. After drying, the yellow crude compound was purified by silica flash chromatography using light petroleum/ethyl acetate (6:4, v:v) as eluent, giving a pale yellow compound in 62% yield. Anal. Calcd. for $C_{32}H_{32}N_2O_6$ (540.62): C 71.11; H 5.97; N 5.18. Found: C 71.00; H 6.03; N 5.25. ^{1}H NMR (300 MHz, $CDCl_3$, 25 °C, TMS): δ = 2.47 (s, 6H, CH_3–N–binaphthyl), 2.63–2.82 (m, 8H, CH_2–CH_2OCO), 3.67 (s, 6H, CH_3OCO), 6.85–7.05 (m, 2H, CH–binaphthyl), 7.20–7.26 (m, 6H, CH–binaphthyl), 7.71–7.86 (m, 4H, CH–binaphthyl). ^{13}C NMR (75.5 MHz, $CDCl_3$, 25 °C, TMS): δ = 29.6, 36.1, 37.9, 52.1, 126.5, 127.0, 127.8, 128.7, 129.3, 130.7, 131.6, 132.6, 134.2, 142.4, 173.2, 174.4. MS (ESI): *m/z* (%) = 540 (100) $[M + 1]^+$.

2.2.5. Butanoic acid, 4-{*N*,*N*′-dimethyl-*N*,*N*′-[(1,1′-binaphthalene)-2,2′diyl]-4-oxo (**5**)

Butanoic acid, 4-{*N*,*N*′-dimethyl-*N*,*N*′-[(1,1′-binaphthalene)-2,2′diyl]-4-oxo, methyl ester (**4**) (0.337 g, 0.62 mmol) was allowed to react with an anhydrous methanolic solution of KOH (0.070 g, 1.24 mmol) at room temperature under stirring for 12 h. Then, the solvent was removed by rotary evaporation and the solid residue, after dissolution in dichloromethane, was quenched with 2N HCl (10 ml). The organic layer was separated and the aqueous layer was extracted with dichloromethane (3 × 20 ml). After drying with Na_2SO_4, the solvent was removed by rotary evaporation, giving a pale yellow powder (78% yield). Anal. Calcd. for $C_{30}H_{28}N_2O_6$ (512.57): C 70.29; H 5.57; N 5.47. Found: C 70.45; H 5.64; N 5.33. ^{1}H NMR (300 MHz, $CDCl_3$, 25 °C, TMS): δ = 2.47 (s, 6H, CH_3–N–binaphthyl, 2.63–2.82 (m, 8H, CH_2–CH_2OCO), 6.85–7.05 (m, 2H, CH–binaphthyl), 7.20–7.26 (m, 6H, CH–binaphthyl), 7.71–7.86 (m, 4H, CH–binaphthyl), 11.0 (s, 2H, COOH). ^{13}C NMR (75.5 MHz, $CDCl_3$, 25 °C, TMS): δ = 29.6, 36.1, 37.9, 126.5, 127.0, 127.8, 128.7, 129.3, 130.7, 131.6, 132.6, 134.2, 142.4, 174.4, 177.3. MS (ESI): *m/z* (%) 512 (100) $[M + 1]^+$.

2.2.6. Butanediamide, *N*,*N*′-dimethyl-*N*,*N*′-[(1,1′-binaphthalene)-2,2′diyl]-*N*″,*N*‴-bis[bis(1-methyl-2-benzimidazolylmethyl)] (**6**)

Butanoic acid, 4-{*N*,*N*′-dimethyl-*N*,*N*′-[(1,1′-binaphthalene)-2,2′diyl]-4-oxo, (5) (0.050 g, 0.0975 mmol), bis[(1-methyl-2-benzimidazolylmethyl)]amine [36] (0.060 g, 0.195 mmol), *O*-(1H-benzotriazol-1-yl)-*N*,*N*,*N*′*N*′-tetramethyluronium hexafluorophosphate (HBTU) (0.082 g, 0.215 mmol), 1-hydroxybenzotriazole (HOBT) (0.029 g, 0.215 mmol) were dissolved, under nitrogen, in an anhydrous mixture of CH_3CN/DMF (1:1, v:v) (6 ml). Triethylamine (Et_3N) (0.059 g, 0.585 mmol) dissolved in anhydrous CH_3CN (2 ml), was then added dropwise within 10 min and the mixture, kept under nitrogen, was stirred at room temperature for 24 h. The reaction was followed by TLC (silica) using dichloromethane/methanol (9:1, v:v) as eluent. After evaporation of the solvent at reduced pressure, the product was treated with a saturated solution of Na_2CO_3 and the aqueous layer was extracted with dichloromethane (3 × 20 ml). The organic layer was dried with Na_2SO_4 and the solvent was removed by rotary evaporation. The crude compound was purified by preparative TLC (silica), upon eluting three times with dichloromethane/methanol (9:1, v:v). The bands of the pure product were scraped out, treated with methanol, and the resulting slurry was filtered off through Celite and washed with methanol. The

organic layers were dried with Na_2SO_4 and the solvent was removed under reduced pressure, giving a pale yellow compound in 65% yield. Anal. Calcd. for $C_{66}H_{62}N_{12}O_4$ (1087.30): C 72.90; H 5.75; N 15.46. Found: C 73.03; H 5.88; N 15.33. ^{1}H NMR (300 MHz, $CDCl_3$, 25 °C, TMS): δ = 2.37–2.42 (m, 8H, CH_2–CH_2–CO), 2.59 (s, 6H, CH_3–N–binaphthyl), 3.72 (s, 12 H, CH_3–N–benzimidazole), 4.46–4.95 (m, 8H, CH_2–benzimidazole), 6.85–7.26 (m, 16H, CH), 7.47–7.55 (m, 4H, CH–binaphthyl), 7.70–7.95 (m, 8H, CH–benzimidazole). ^{13}C NMR (75.5 MHz, $CDCl_3$, 25 °C, TMS): δ = 29.6, 36.1, 37.9, 52.1, 109.4, 113.7, 120.0, 121.4, 122.4, 123.1, 124.3, 126.4, 126.5, 128.8, 129.1, 129.6, 130.5, 134.6, 136.4, 142.4, 150.7, 151.7, 172.2, 174.4. MS (ESI): *m/z* (%) 1087 (100) $[M + 1]^+$.

2.2.7. *(R)-N,N′-Dimethyl-N,N′-bis{4-[bis(1-methyl-2-benzimidazolylmethyl)]-aminobutyl}-1,1′-binaphthyl-2,2′-diamine, (R)-DABN-4Bz$_4$*

A solution of $BH_3.Me_2S$ (3.32 ml, 34 mmol) in dry THF (10 ml) was added dropwise to a suspension of 6 (0.37 g, 0.34 mmol) in boiling, dry THF (10 ml) under nitrogen. Then, the solvent and Me_2S were slowly distilled during 5 h while adding dry THF (50 ml) dropwise. The solvents were removed under vacuum and the solid residue was taken up with a saturated solution of HCl in methanol. The suspension was refluxed under stirring for 1 h until the solid was completely dissolved. After cooling, the solution was evaporated and the residue was treated with saturated Na_2CO_3 solution until a basic pH was reached. The aqueous layer was extracted with dichloromethane (3 × 20 ml) and the organic layer was dried with Na_2SO_4. Then the solvent was removed under reduced pressure, giving a pale violet oil in 56% yield. Anal. Calcd. for $C_{66}H_{70}N_{12}$ (1031.36): C 76.85; H 6.84; N 16.31. Found: C 76.54; H 6.90; N 16.17. ^{1}H NMR (300 MHz, $CDCl_3$, 25 °C, TMS): δ = 1.37–1.55 (m, 8H, CH_2–CH_2), 2.36 (t, 4H, CH_2–N–CH_2–benzimidazole), 2.69 s, 6H, CH_3–N–binaphthyl), 3.35 (t, 4H, CH_2–N–binaphthyl), 3.72 (s, 12H, CH_3–N–benzimidazole), 4.46–4.95 (m, 8H, CH_2–benzimidazole), 6.85–7.26 (m, 16H, CH), 7.47–7.55 (m, 4H, CH–binaphthyl), 7.70–7.95 (m, 8H, CH–benzimidazole). ^{13}C NMR (75.5 MHz, $CDCl_3$, 25 °C, TMS): δ = 25.4, 26.1, 36.1, 37.9, 49.0, 52.1, 109.4, 113.7, 120.0, 121.4, 122.4, 123.1, 124.3, 126.0, 126.5, 128.8, 129.1, 129.6, 130.5, 134.6, 136.4, 142.4, 150.7, 151.7. An unambiguous assignment of the ^{1}H and ^{13}C signals was obtained from the combination of ^{1}H–^{13}C HMQC, ^{1}H–^{1}H COSY, DEPT135, and ^{1}H–^{13}C HMBC spectra. MS (ESI): *m/z* (%) 1031 (100) $[M + 1]^+$. UV–vis (CH_3CN): λ_{max} (nm) (ε (M cm)$^{-1}$) = 214 (135,000), 224 sh (98,000), 256 (52,500), 268 (43,900), 286 (28,300), 306 sh (19,300), 348 (7700). CD (CH_3CN): λ_{max} (nm) ($\Delta\varepsilon$ (M cm)$^{-1}$) = 214 (+71.4), 224 (−74.0), 265 (−28.3), 280 sh (−5.4), 299 (+4.9), 336 sh (−5.4), 368 (−9.7).

The ligand (*S*)-*N*2,*N*6-dimethyl-*N*2,*N*6-bis{2′-[bis(1-methyl-2-benzimidazolylmethyl)]-aminomethyl}benzyl-2,6-diamino-1-exanol acetate, L-Lys-4Bz$_4$ was prepared following the synthetic route outlined in Fig. 2.

2.2.8. L-*Lysine, N2,N6-diethoxycarbonyl, ethyl ester (**10**)*

L-Lysine dihydrochloride (4.3 g, 17.4 mmol) was suspended in dry, cooled (0 °C) dichloromethane (50 ml). Then, gaseous NH_3 was bubbled into the mixture under stirring. The resulting precipitate was filtered off and the filtrate was concentrated. The precipitate was submitted twice to the same treatment and the filtrates, after evaporation of the solvent, afforded the free amino acid (**9**) (3.0 g, 17.22 mmol), which was dissolved in a mixture of H_2O/EtOH/pyridine (60:32:8, v:v:v) (150 ml). After cooling this solution in an ice bath, ethyl chloroformate (10.64 g, 112.0 mmol) was added dropwise, under nitrogen, during 30 min. The mixture was then warmed to room temperature and stirred for 48 h. The reaction, followed by TLC (silica) using light petroleum/ethyl acetate (6:4, v:v) as eluent, was concentrated and quenched by the addition of 2N HCl (40 ml), and finally extracted with dichloromethane (4 × 40 ml). The organic layers were dried with Na_2SO_4 and the solvent was removed by rotary evaporation. The oily residue was purified by silica flash chromatography (3 × 20 cm) in the following conditions: pressure, 2 inch/min; eluent, light petroleum/ethyl acetate starting from 7:3 (v:v) to 1:9 (v:v) (each fraction 100 ml). The fractions containing the pure compound were evaporated, furnishing a pale yellow oil in 70% yield. Anal. Calcd. for $C_{14}H_{26}N_2O_6$ (318.37): C 52.81; H 8.23; N 8.80. Found: C 52.96; H 8.35; N 8.68. ^{1}H NMR (300 MHz, $CDCl_3$, 25 °C, TMS): δ = 1.25 (t, 9H, CH_3–CH_2), 1.40 (m, 2H, CH_2–NH), 1.55 (m, 2H, CH_2–CH_2), 1.75 (m, 2H, CH_2–NH), 3.10 (m, 2H, CH_2–NH), 4.15 (q, 6H, CH_3–CH_2), 4.30 (m, 1H, CH), 4.70 (s, 1H, NH), 5.24 (s, 1H, NH). ^{13}C NMR (75.5 MHz, $CDCl_3$, 25 °C, TMS): δ = 14.5, 15.0, 22.6, 31.3, 32.7, 40.8, 53.9, 61.2, 61.3, 156.9, 172.9. MS (ESI): *m/z* (%) 319 (100) $[M + 1]^+$.

2.2.9. *N2,N6-dimethyl-2,6-diamino-1-hexanol (**11**)*

$LiAlH_4$ (1.51 g, 37.95 mmol) was suspended in dry THF (50 ml) under nitrogen and cooled to 0 °C. The dicarbamate 10 (2.35 g, 7.95 mmol) dissolved in dry THF (15 ml) was then slowly added via a dropping funnel and the mixture was warmed and then refluxed for 24 h. The reaction was followed by TLC (alumina) using CH_2Cl_2/MeOH (9:1, v:v) as eluent. After cooling to room temperature and then to 0 °C, excess of $LiAlH_4$ was quenched with MeOH (2 ml), NaOH 15% (2 ml) and finally H_2O (5 ml). The gray precipitate was filtered through Celite and washed several times with diethyl ether. The filtrate and washings were combinated and evaporated under reduced pressure, giving an orange–yellow oil (yield 82.2%). Anal. Calcd. for $C_8H_{20}N_2O$ (160.26): C 59.95; H 12.58; N 17.48. Found: C 60.07; H 12.78; N 17.33. ^{1}H NMR (300 MHz, CD_3OD, 25 °C, TMS): δ = 1.40 (m, 2H, CH_2), 1.45 (m, 2H, CH_2), 1.54 (m,

2H, CH_2), 2.38 (s, 6H, CH_3–NH), 2.48 (m, 1H, CH–NH), 2.55 (t, 2H, CH_2–NH), 3.44–3.60 (m, 2H, CH_2–OH). ^{13}C NMR (75.5 MHz, $CDCl_3$, 25 °C, TMS): δ = 23.8, 29.6, 30.5, 32.6, 35.2, 51.6, 62.1, 62.7. MS (ESI): *m/z* (%) 161 (100) $[M + 1]^+$.

2.2.10. *N2,N6-dimethyl-N2,N6-bis(2′-cyano)benzyl-2,6-diamino-1-hexanol* (**12**)

To a solution of compound **11** (0.503 g, 3.14 mmol) in dry CH_3CN (50 ml) was added, under nitrogen, 2-(bromomethyl)benzonitrile (Aldrich) (1.36 g, 6.97 mmol) and anhydrous K_2CO_3 (1.31 g, 9.50 mmol) and the resulting mixture was stirred at room temperature for 48 h. The reaction was followed by TLC (silica) using dichloromethane/ethyl acetate (1:1, v:v) as eluent. After filtration, the solvent was removed under reduced pressure and the yellow oil was purified by silica flash chromatography (3 × 20 cm) in the following conditions: pressure, 1 in./min; eluent, dichloromethane/ethyl acetate starting from 1:1 (v:v) (500 ml) to pure ethyl acetate (500 ml). The fractions containing the pure product were evaporated to dryness, furnishing a white compound in 48% yield. Anal. Calcd. for $C_{24}H_{30}N_4O$ (390.52): C 73.81; H 7.74; N 14.35. Found: C 73.54; H 7.85; N, 14.23. ^1H NMR (300 MHz, $CDCl_3$, 25 °C, TMS): δ = 1.15 (m, 2H, CH_2), 1.34 (m, 2H, CH_2–N), 1.56 (m, 2H, CH_2–CH_2), 2.24 (s, 6H, CH_3–N), 2.47 (m, 2H, CH_2–N–CH_3–benzyl), 2.75 (m, 1H, CH–CH_2), 3.35–3.55 (m, 2H, CH_2–OH), 3.69 (s, 4H, CH_2–benzyl), 7.37–7.66 (m, 8H, CH–benzyl). ^{13}C NMR (75.5 MHz, $CDCl_3$, 25 °C, TMS): δ = 35.7, 42.4, 60.5, 113.2, 118.4, 128.1, 130.5, 133.1, 133.5, 143.8. MS (ESI): *m/z* (%) 391 (100) $[M + 1]^+$.

2.2.11. *N2,N6-dimethyl-N2,N6-bis(2′-aminomethyl) benzyl-2,6-diamino-1-hexanol* (**13**)

$LiAlH_4$ (0.30 g, 7.90 mmol) was suspended in dry THF (40 ml) under N_2 and cooled to 0 °C. The dicyano derivative 12 (0.28 g, 0.72 mmol) dissolved in dry THF (10 ml) was then slowly added via a dropping funnel and the mixture was warmed and then refluxed for 24 h. The reaction was followed by TLC (alumina) using CH_2Cl_2/MeOH (7:3, v:v) as eluent. Proceeding in a similar way as for compound **11**, a red oil was obtained (84.5% yield). Anal. Calcd. for $C_{24}H_{38}N_4O$ (398.59): C 72.31; H 9.61; N 14.06. Found: C 72.11; H 9.80; N 13.95. ^1H NMR (300 MHz, $CDCl_3$, 25 °C, TMS): δ = 1.32 (m, 2H, CH_2–CH_2–N–CH_2OH), 1.34 (m, 2H, CH_2–N–CH_2OH), 1.56 (m, 2H, CH_2–N–CH_3), 2.16 (s, 6H, CH_3–N), 2.43 (m, 2H, CH_2–N–CH_3), 2.65 (m, 1H, CH–CH_2OH), 3.54 (s, 4H, CH_2–benzyl), 3.58–3.64 (m, 2H, CH_2OH), 3.79 (s, 4H, CH_2–NH_2), 7.24–7.33 (m, 8H, CH–benzyl). ^{13}C NMR (75.5 MHz, $CDCl_3$, 25 °C, TMS): δ = 25.3, 26.0, 27.5, 34.9, 41.0, 43.6, 57.6, 61.2, 62.5, 63.5, 126.9, 129.5, 131.3, 137.4, 141.6. MS (ESI): *m/z* (%) 399 (100) $[M + 1]^+$.

2.2.12. *N2,N6-dimethyl-N2,N6-bis{2′-[bis(1-methyl-2-benzimidazolylmethyl)]aminomethyl}benzyl-2,6-diamino-1-exanol* (**14**)

Compound **13** (0.106 g, 0.265 mmol) was dissolved in dry acetonitrile (10 ml). 2-(Chloromethyl)-1-methylbenzimidazole (0.201 g, 1.11 mmol) [24], and dry sodium carbonate (0.15 g, 1.42 mmol) were then added and the stirred mixture was refluxed for 6 h under N_2. The reaction was followed by TLC (alumina) using CH_2Cl_2/MeOH (7:3, v:v) as eluent. The mixture was cooled and the precipitate so obtained was filtered off; it consists of a mixture of product and inorganic salts and was thus treated with $CHCl_3$ and filtered again. The combined filtrates were dried under vacuum to afford a yellow powder in 84% yield. Anal. Calcd. for $C_{60}H_{70}N_{12}O$ (975.28): C 73.89; H 7.23; N 17.24. Found: C 73.54; H 7.12; N 17.38. ^1H NMR (300 MHz, $CDCl_3$, 25 °C, TMS): δ = 0.88 (m, 2H, CH_2–CH_2–N–CH_2OH), 1.02 (m, 2H, CH_2–N–CH_2OH), 1.27 (m, 2H, CH_2–CH_2–CH_2–N–CH_3), 2.01 (m, 2H, CH_2–CH_2–CH_2–CH_2–N–CH_3), 2.05 (s, 6H, CH_3–N–CH_2), 2.22 (m, 1H, CH–CH_2OH), 3.22 (s, 12H, CH_3–N–benzimidazole), 3.41 (m, 4H, CH_2–N–CH_3), 3.58–3.76 (m, 2H, CH_2OH), 4.01 (m, 4H, CH_2–N), 7.01 (m, 8H, CH_2–C–benzimidazole), 7.23 (m, 8H, CH–benzimidazole), 7.26–7.39 (m, 8H, CH–benzyl), 7.72 (m, 8H, CH–benzimidazole). ^{13}C NMR (75.5 MHz, $CDCl_3$, 25 °C, TMS): δ = 24.0, 25.7, 27.5, 29.2, 35.5, 40.2, 55.3, 56.3, 59.8, 63.2, 109.3, 119.5, 122.2, 123.0, 127.3, 128.3, 130.5, 131.7, 136.6, 139.8, 142.8, 152.1. MS (ESI): *m/z* (%) 975 (100) $[M + 1]^+$.

2.2.13. *(S)-N2,N6-dimethyl-N2,N6-bis{2′-[bis(1-methyl-2-benzimidazolylmethyl)]aminomethyl} benzyl-2,6-diamino-1-exanol acetate,* L-*Lys-4Bz*$_4$

Compound **14** (0.207 g, 0.212 mmol) was dissolved in acetic anhydride (10 ml). *N,N*-Dimethylpyridin-4-amine (0.0156 g, 0.127 mmol) was then added and the mixture was stirred at room temperature for 12 h. The solvent was removed under reduced pressure and the yellow–orange oil was purified by silica flash chromatography using CH_2Cl_2/MeOH (from 97:3 to 60:40, v:v, 100 ml) as gradient. The fractions of pure product were evaporated under vacuum, furnishing a yellow powder (98% yield). Anal. Calcd. for $C_{62}H_{72}N_{12}O_2$ (1017.32): C 73.19; H 7.13; N 16.52. Found C 73.23; H 7.21; N 16.68. ^1H NMR (300 MHz, $CDCl_3$, 25 °C, TMS): δ = 0.88 (m, 2H, CH_2–CH_2–N–CH_2OCO), 1.02 (m, 2H, CH_2–N–CH_2OCO), 1.27 (m, 2H, CH_2–CH_2–CH_2–N–CH_3), 2.01 (m, 2H, CH_2–CH_2–CH_2–CH_2–N–CH_3), 2.03 (s, 3H, CH_3–CO), 2.05 (s, 6H, CH_3–N–CH_2), 2.22 (m, 1H, CH–CH_2OCO), 3.22 (s, 12H, CH_3–N–benzimidazole), 3.41 (m, 4H, CH_2–N–CH_3), 3.58–3.76 (m, 2H, CH_2OCO), 4.01 (m, 4H, CH_2–N), 7.01 (m, 8H, CH_2–C–benzimidazole), 7.23 (m, 8H, CH–benzimidazole), 7.26–7.39 (m, 8H, CH–benzyl), 7.72 (m, 8H, CH–benzimidazole). ^{13}C NMR (75.5 MHz, $CDCl_3$, 25 °C, TMS): δ = 21.2, 24.0, 25.7, 29.2, 35.5, 40.2, 55.3, 56.3, 56.8, 59.8, 63.2, 109.3, 119.5, 122.2, 123.0, 127.3,

128.3, 130.5, 131.7, 136.6, 139.8, 142.8, 152.1, 171.9. An unambiguous assignment of the ^{1}H and ^{13}C signals was obtained from the combination of ^{1}H–^{13}C HMQC, ^{1}H–^{1}H COSY, DEPT135, and ^{1}H–^{13}C HMBC spectra. MS (ESI): *m/z* (%) 1017 (100) $[M+1]^{+}$. UV–vis (CH_3CN): λ_{max} (nm) (ε (M cm)$^{-1}$) = 250 sh (31,500), 256 (33,600), 270 (28,200), 278 (29,200), 285 (32,000). CD (CH_3CN): λ_{max} (nm) ($\Delta\varepsilon$ (M cm)$^{-1}$) = 256 (−1.45).

2.3. Syntheses of the copper(II) complexes

2.3.1. $[Cu_2DABN\text{-}3Im_4][ClO_4]_4\cdot 6H_2O$

To a solution of the ligand (*R*)-DABN-3Im$_4$ (0.209 g, 0.26 mmol) in MeOH (10 ml), copper(II) perchlorate hexahydrate (0.193 g, 0.52 mmol) was added. The resulting green solution was stirred at room temperature and after few minutes a green precipitate was observed. The mixture was evaporated to a small volume (2–3 ml) and treated with diethyl ether (2 ml). The green product was filtered, washed with water (1 ml) and dried under vacuum (93.0% yield). Anal. Calcd. for $C_{48}H_{58}N_{12}O_{16}Cu_2Cl_4\cdot 6H_2O$ (1436.05): C 40.14; H 4.91; N 11.71; Cu 8.85. Found: C 40.14; H 5.02; N 11.56; Cu 8.91. UV–vis (CH_3CN): λ_{max} (nm) (ε (M cm)$^{-1}$) = 218 (85,900), 250 (52,300), 290 sh (18,400), 300 (15,800), 348 (7300), 690 (100). CD (CH_3CN): λ_{max} (nm) ($\Delta\varepsilon$ (M cm)$^{-1}$) = 213 (+61.8), 224 (−31.6), 257 (−38.2), 297 (+8.5), 326 (+2.5), 372 (−1.8), 600 (−0.02), 710 (+0.08).

The dinuclear complexes $[Cu_2DABN\text{-}4Bz_4][ClO_4]_4$ and $[Cu_2Lys\text{-}4Bz_4][ClO_4]_4$ were obtained in a similar way as above reported for $[Cu_2DABN\text{-}3Im_4][ClO_4]_4$.

2.3.2. $[Cu_2DABN\text{-}4Bz_4][ClO_4]_4\cdot 2H_2O$

Anal. Calcd. for $C_{66}H_{70}N_{12}O_{16}Cu_2Cl_4\cdot 2H_2O$ (1592.25): C 49.78; H 4.68; N 10.56; Cu 7.98: Found: C 49.85; H 4.78; N 10.71; Cu 8.03. UV–vis (CH_3CN): λ_{max} (nm) (ε (M cm)$^{-1}$) = 214 (122,000), 232 (62,000), 256 (42,300), 272 (39,000), 280 (34,100), 306 sh (14,700), 352 (6800), 434 (1700), 524 (1700), 662 (184). CD (CH_3CN): λ_{max} (nm) ($\Delta\varepsilon$ (M cm)$^{-1}$) = 213 (+62.8), 224 (−59.8), 264 (−23.6), 295 (+5.8), 334 sh (+0.5), 367 (−2.6).

2.3.3. $[Cu_2Lys\text{-}4Bz_4][ClO_4]_4\cdot 6H_2O$

Anal. Calcd. for $C_{62}H_{72}N_{12}O_{18}Cu_2Cl_4\cdot 6H_2O$ (1650.29): C 45.12; H 5.13; N 10.19; Cu 7.70. Found: C 44.97; H 5.21; N 9.99; Cu 7.73. UV–vis (CH_3CN): λ_{max} (nm) (ε (M cm)$^{-1}$) = 245 (25,300), 255 sh (24,000), 265 sh (23,900), 272 (29,300), 280 (27,900), 306 sh (2850), 378 sh (650), 662 (180).

2.3.4. $[Cu_3DABN\text{-}3Im_4][ClO_4]_6\cdot 2H_2O$

To a solution of the ligand (*R*)-DABN-3Im$_4$ (0.285 g, 0.355 mmol) in MeCN (10 ml), a solution of copper(II) perchlorate hexahydrate (0.434 g, 1.17 mmol) dissolved in MeOH (2 ml) was added. The resulting green–brown solution was refluxed under stirring for 24 h. The mixture was then cooled to room temperature and evaporated to a small volume (2–3 ml), while MeOH (10 ml) was added in three times. The deep green product thus obtained was filtered, washed with water (1 ml) and dried under vacuum (54.0% yield). Anal. Calcd. for $C_{48}H_{58}N_{12}O_{24}Cu_3Cl_6\cdot 2H_2O$ (1626.47): C 35.44; H 4.03; N 10.34; Cu 11.72. Found: C 35.74; H 4.11; N 10.27; Cu 11.83. UV–vis (CH_3CN): λ_{max} (nm) (ε (M cm)$^{-1}$) = 216 (103,000), 252 (57,000), 280 sh (39,400), 306 sh (27,900), 358 (20,000), 374 (19,400), 662 (204). CD (CH_3CN): λ_{max} (nm) ($\Delta\varepsilon$ (M cm)$^{-1}$) = 212 (+18.7), 223 (−8.2), 237 (−12.3), 286 (+4.34), 350 (−0.93), 384 (+0.75), 510 (−0.36), 688 (+0.19).

The trinuclear complexes $[Cu_3DABN\text{-}4Bz_4][ClO_4]_6$ and $[Cu_3Lys\text{-}4Bz_4][ClO_4]_6$ were obtained in a similar way as above reported for $[Cu_3DABN\text{-}3Im_4][ClO_4]_6$.

2.3.5. $[Cu_3DABN\text{-}4Bz_4][ClO_4]_6\cdot 2H_2O$

Anal. Calcd. for $C_{66}H_{70}N_{12}O_{24}Cu_3Cl_6\cdot 2H_2O$ (1854.75): C 42.74; H 4.02; N 9.06; Cu 10.28. Found: C 42.94; H 4.13; N 9.15; Cu 10.36. UV–vis (CH_3CN): λ_{max} (nm) (ε (M cm)$^{-1}$) = 212 (107,000), 254 (62,400), 274 (57,200), 280 (45,500), 304 sh (24,000), 356 sh (9050), 414 sh (6300), 460 sh (7200), 484 (8800), 526 (6800), 718 (174). CD (CH_3CN): λ_{max} (nm) ($\Delta\varepsilon$ (M cm)$^{-1}$) = 212 (+70.6), 224 (−63.5), 258 (−36.8), 298 (+4.2), 344 (+4.6), 379 (−1.2), 532 (−0.2).

2.3.6. $[Cu_3Lys\text{-}4Bz_4][ClO_4]_6\cdot 6H_2O$

Anal. Calcd. for $C_{62}H_{72}N_{12}O_{26}Cu_3Cl_6\cdot 6H_2O$ (1912.73): C 38.93; H 4.43; N 8.79; Cu 9.96. Found: C 38.53; H 4.76; N 8.88; Cu 10.01. UV–vis (CH_3CN): λ_{max} (nm) (ε (M cm)$^{-1}$) = 245 (20,300), 265 sh (15,500), 272 (18,500), 280 (17,800), 286 sh (9900), 312 sh (2560), 380 sh (433), 573 (170), 660 (60).

However, perchlorate complexes with organic ligands are potentially explosive and should be handled with great care. Only small amounts of material should be prepared. We did not have problems working with small amounts of the perchlorate complexes described in this paper.

2.4. Catalytic oxidations of 3,5-di-tert-butylcatechol, L-/D-Dopa, and L-/D-Dopa methyl esters

The kinetics of catalytic oxidation of 3,5-di-*tert*-butylcatechol were studied by UV–vis spectroscopy using a magnetically stirred and thermostated 1-cm path length cell. The temperature during the measurements was kept constant at 20 ± 0.1 °C. A mixture of methanol-aqueous phosphate buffer (50 mM, pH 5.0) 30:1 (v:v) saturated with atmospheric oxygen was used as solvent. All the kinetic experiments were carried out in triplicate. The experiments carried out over a substrate concentration range were initiated by adding a few microlitres of the complexes (final concentrations 1.1–1.6 × 10^{-5} M) to the solution of DTBC; the concentration of the substrate was varied between 7.0 × 10^{-5} and 1.2 × 10^{-2} M (final volume 2 ml). The formation of 3,5-di-*tert*-butylquinone was followed monitoring the increase of absorbance at λ_{max} = 400 nm, corresponding to a characteris-

tic band of the product (ε_{400} = 1500 (M cm)$^{-1}$) in methanol). The oxidations followed a biphasic behaviour; the rate of the first step was obtained from the slope of the curve of absorbance versus time in the first few seconds of the reaction, while the rate of the second step was calculated from the linear plot corresponding to the second, catalytic phase. The noise during the experiments was reduced by reading the absorbance difference between 400 and 800 nm, where the absorption remains negligible during the assay.

The catalytic oxidations of the substrates L-, D-Dopa, and L-, D-Dopa methyl esters (L-, D-DopaOMe) were studied by UV–vis spectroscopy, using a mixture of methanol-aqueous phosphate buffer (50 mM, pH 8.5) 1:15 (v:v), saturated with atmospheric oxygen, as solvent. The experiments were carried out using the same equipment as before at the constant temperature of 20 ± 0.1 °C. The copper catalyst concentration was in the range 2.0–5.2 × 10^{-6} M (final concentration) in all the experiments, while the substrate concentration was varied from 3.9 × 10^{-6} to 8.0 × 10^{-4} M (final volume 2 ml). To prevent further reactions of the quinones initially formed, an excess amount of 3-methyl-2-benzothiazoline hydrazone (MBTH, 1.0 × 10^{-3} M) was added, as we did before [31,33,34]. The formation of the stable Dopa-*o*-quinone-MBTH and DopaOMe-*o*-quinones-MBTH adducts was followed through the development of the strong absorption band at 500 nm (ε_{500} = 13,400 (M cm)$^{-1}$ for Dopa-*o*-quinone-MBTH, and ε_{500} = 11,600 (M cm)$^{-1}$ for DopaOMe-*o*-quinone-MBTH, respectively). As before, in all the experiments, the noise was reduced by reading the absorbance difference between 500 and 800 nm, and the initial rate of the oxidations were obtained by fitting the absorbance versus time curves in the first few seconds of the reactions.

3. Results and discussion

3.1. Ligand design and synthesis

The synthesis of the ligand (*R*)-DABN-3Im$_4$ was carried out by condensation of a slight excess of 2-(chloromethyl)-1-methylimidazole with intermediate 8. The multistep procedure to obtain the diamine 8 was reported previously [32]. The use of *N*-methylated imidazoles, as for benzimidazoles, increases the chemical stability of the resulting metal complexes in the oxidative reactions. In order to obtain the ligand (*R*)-DABN-4Bz$_4$, several methods were applied for the activation of secondary amine groups of (*R*)-*N*,*N*′-dimethyl-1,1′-binaphthyl-2,2′-diamine, **3**, either by refluxing this intermediate in chloroform with succinic anhydride for 3 days, also in the presence of *N*,*N*-dimethylpyridin-4-amine (DMP) or Et$_3$N, or mixing compound **3** with ethyl 4-bromobutanoate in DMF at 80 °C for 10 h. Other experiments were carried out with 4-methoxy-4-oxobutanoic acid in acetonitrile with HBTU, HOBT, and Et$_3$N, but in all these cases, the product mixtures showed the presence of several by-products and unreacted reagents even after long reaction time. A more promising approach was found when compound **3** was treated with methyl 4-chloro-4-oxobutanoate in dichloromethane in the presence of triethylamine as a base (Fig. 1). In this way, compound **4** was produced, which was transformed into the corresponding diacid 5. Compound **5** was then treated with bis[(1-methyl-2-benzimidazolylmethyl)]amine [36], in acetonitrile-dimethylformamide solution and in the presence of HOBT, HBTU and triethylamine, to give compound **6**. Reduction of the carbonyl groups with BH$_3$.Me$_2$S, in tetrahydrofuran solution, led to the ligand (*R*)-DABN-4Bz$_4$, where carbon chains of four carbon atoms separating the tridentate nitrogen donors from the chiral spacer are present, instead of three as in the previous octadentate ligands. We expect that lengthening these carbon chains will prevent the interaction of the tertiary nitrogen donors of the 1,1-binaphthyl residue in the dinuclear complex and facilitate the binding of the third copper(II) ion in the trinuclear complex.

The reactions reported in Fig. 2 proved to be a valid method for the preparation of the ligand L-Lys-4Bz$_4$. The free ethyl ester amino acid (**9**) was treated with two molecules of ethyl chloroformate to give the corresponding dicarbamate 10, which was reduced to compound **11**. Condensation of **11** with 2-bromomethyl benzonitrile led to compound **12**, which was reduced to compound **13**. Compound **13** was treated with an excess of 2-(chloromethyl)-1-methylbenzimidazole to afford **14** and then *O*-acetylated to give L-Lys-4Bz$_4$.

3.2. Optical and CD spectroscopy

The electronic spectra of (*R*)-DABN-3Im$_4$ and (*R*)-DABN-4Bz$_4$ are qualitatively similar to that of the parent (*R*)-DABN-3Bz$_4$ derivative [32], with somewhat lower intensity for some of the bands in the case of (*R*)-DABN-3Im$_4$, due to the presence of imidazole rather than benzimidazole groups. The CD spectra of the new ligands are dominated by the features of the chiral 1,1′-binaphthyl chromophore. For both (*R*)-DABN-3Im$_4$ and (*R*)-DABN-4Bz$_4$, negative CD couplets are observed between 200 and 240 nm, which ensure that the naphthalene rings maintain a cisoid conformation (with *M* helicity) as their parent derivatives [32,37]. There are important differences, though, between the CD spectra of (*R*)-DABN-3Im$_4$ and (*R*)-DABN-4Bz$_4$ and that of (*R*)-DABN-3Bz$_4$. The CD couplets of the former compounds are in fact of lower intensity and the spectra further lack the distinctive CD feature at 248 nm indicating, for (*R*)-DABN-3Bz$_4$, an unusually reduced dihedral angle between the naphthalene rings (computed to be about 75°) [32]. This peculiar conformation was previously observed only for chain-bridged 1,1′-binaphthyl derivatives [37] and, in the case of (*R*)-DABN-3Bz$_4$, it is imposed by ring stacking interactions between the naphthalene rings and the benzimidazole rings [32]. Clearly, lengthening the carbon chains separating the naphthalene rings from the benzimidazoles, as in (*R*)-DABN-4Bz$_4$, or replacing the benzimidazoles with the smaller imidazoles, as in (*R*)-DABN-3Im$_4$, is unable to maintain such stacking interactions and,

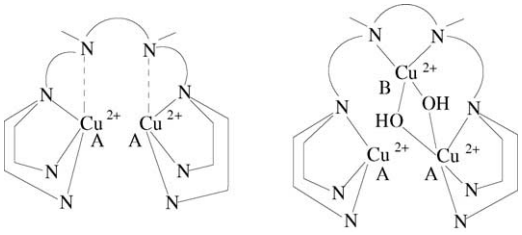

Scheme 1. Proposed schematic structures for the dinuclear and trinuclear complexes.

therefore, the conformational arrangement of the naphthalene rings in the new ligands corresponds to that of unstrained 1,1′-binaphthyl chromophores, which typically involves dihedral angles around 90° [37].

The CD spectra of the copper(II) complexes $[Cu_2DABN\text{-}3Im_4]^{4+}$ and $[Cu_3DABN\text{-}3Im_4]^{6+}$ exhibit some significant differences. In the far-UV region, the exciton doublet centred at 200–240 nm has reduced intensity in the spectrum of the dinuclear compound with respect to the free ligand, and is basically absent in that of the trinuclear complex. The situation is quite similar to that discussed previously for the corresponding complexes in the (*R*)- and (*S*)-DABN-$3Bz_4$ series [31,32,34], and is due to changes in the dihedral angle between the naphthalene rings, that in the trinuclear complex are likely severely distorted towards coplanarity to accommodate a Cu(II) ion in site B (Scheme 1). The CD spectrum of $[Cu_2DABN\text{-}3Im_4]^{4+}$ additionally differs from that of (*R*)-DABN-$3Im_4$ in the 250–400 nm region, due to the presence of LMCT transitions, and for the presence of low-energy LF bands. The negative CD peak and 257 nm is more intense than the corresponding peak for the free ligand and two peaks of opposite sign at 326 and 372 nm replace the broad ligand CD band centred at 375 nm. The presence of weak CD activity in the LF bands suggests that the binaphthyl amine groups are at least weakly interacting with the Cu(II) centres, as found for the parent dinuclear complex in the DABN-$3Bz_4$ series [31,34]. The CD spectrum of $[Cu_3DABN\text{-}3Im_4]^{6+}$ displays in the near-UV region a couple of bands of opposite sign at 350 and 384 nm, corresponding to a pair of peaks of considerable intensity in the electronic spectrum (at 358 and 374 nm), which are completely absent in the spectra of $[Cu_2DABN\text{-}3Im_4]^{4+}$. Similar spectral features were encountered also for $[Cu_3DABN\text{-}3Bz_4]^{6+}$ and were attributed to hydroxo → Cu(II) LMCT transitions from dissociated water molecules bound as bridging ligands between one of the Cu(II) centres at site A and that at site B (Scheme 1) [34]. The latter Cu(II) ion is close to the chiral binaphthyl group and is mostly responsible for the significant CD activity of the trinuclear complex in the visible region, which is stronger than for the dinuclear complex.

Regarding the Cu(II) complexes derived from (*R*)-DABN-$4Bz_4$, the most striking behaviour is exhibited by $[Cu_3DABN\text{-}4Bz_4]^{6+}$. Unlike all the parent trinuclear copper complexes in the series, the CD spectrum of this compound features a prominent CD couplet in the 200–240 nm range, with intensity similar to that found for both the free ligand and $[Cu_2DABN\text{-}4Bz_4]^{4+}$. Clearly, here the longer carbon chains allow the binaphthyl residue to bind the Cu(II) ion at site B without distortion of the dihedral angle between the two naphthalene rings. In addition, while the CD spectra of $[Cu_2DABN\text{-}4Bz_4]^{4+}$ and $[Cu_3DABN\text{-}4Bz_4]^{6+}$ are qualitatively similar throughout the near-UV spectral range, that of dinuclear complex is flat in the LF region, indicating that the longer carbon chain of the ligand now prevents significant interaction between the binaphthyl amine groups and the Cu(II) centres. A further spectral feature to note is a prominent multicomponent absorption band near 484 nm in the spectrum of complex $[Cu_3DABN\text{-}4Bz_4]^{6+}$. In spite of the red shift, we believe that this band corresponds to those observed for $[Cu_3DABN\text{-}3Bz_4]^{6+}$ [34], and $[Cu_3DABN\text{-}3Im_4]^{6+}$ in the 350–400 nm range, and attribute it to hydroxo-Cu(II) LMCT transitions, from at least one bridging hydroxo group. The red shift is probably caused by the different stereochemistry at the Cu(II) sites, as is indicated by the different position of the LF bands in the optical spectra.

The UV spectrum of L-Lys-$4Bz_4$ exhibits much weaker absorption bands in the UV region (at 250, 256, 270, 278, and 285 nm) than the ligands in the 1,1′-binaphthyl series. These bands are attributable to the xylyl and benzimidazole chromophores, and only that at 256 nm (likely due to xylyl) is dichroic. The corresponding complexes $[Cu_2Lys\text{-}4Bz_4]^{4+}$ and $[Cu_3Lys\text{-}4Bz_4]^{6+}$ exhibit similar pattern of electronic bands in the aromatic region, with additional features near 380 nm and LF bands at lower energy. The CD spectra of these compounds are featureless throughout the spectral range.

In general, the LF bands of the Cu(II) complexes fall in the range between 650 and 720 nm, which is similar to that reported previously for the parent Cu(II)-DABN-$3Bz_4$ complexes [31,34], and is therefore indicative of tetragonal stereochemistries at the Cu(II) centres, most likely with five-coordinate structures, as deduced for the parent complexes on the basis of a more detailed spectroscopic analysis. In the case of $[Cu_3Lys\text{-}4Bz_4]^{6+}$, the LF spectrum exhibits two maxima at 573 and 660 nm. The latter absorption occurs also in the spectrum of $[Cu_2Lys\text{-}4Bz_4]^{4+}$ and can be attributed to the Cu(A) centres, therefore the band at 573 nm must be attributed to the Cu(B) centre.

3.3. Catalytic oxidation of 3,5-di-tert-butylcatechol

The catalytic oxidation of catechols is the most widely employed test reaction to investigate the behaviour of tyrosinase or catechol oxidase model complexes. Among the various catechols used in these studies [1], 3,5-di-*tert*-butylcatechol (DTBC) is the generally preferred substrate, due to its low redox potential, which makes it easy to oxidize to 3,5-di-*tert*-butylquinone (DTBQ), and the presence of bulky, nonpolar substituents, which prevent further oxidation reactions, such as ring opening reactions, and cyclization/tautomerization reactions. The plots of the initial rates of oxidation of DTBC as a function of substrate concentration exhibited saturation be-

haviour, while a linear relationship between the rates and the concentration of the complexes, indicating first order dependence, was found for all the compounds studied in this work. The reactivity experiments were performed in the mixed solvent methanol/aqueous 50 mM phosphate buffer (pH 5.0) saturated with atmospheric oxygen, as we did before with the complexes of (*R*)-DABN-3Bz$_4$ [31]. Previous studies carried out by our group [27–29,38,39], have demonstrated that the mechanism of catechol oxidation occurs in two steps, where an initial, fast stoichiometric step (reaction 1) is followed by a slower catalytic reaction (reaction 2), according to the following simplified scheme:

$$Cu_2^{II} + DTBC \rightleftharpoons [Cu_2^{II}DTBC] \rightarrow Cu_2^{I} + DTBQ + 2H^+ \quad (1)$$

$$Cu_2^{I} + DTBC + O_2 \rightleftharpoons [Cu_2^{I}\text{–}O_2\text{–}DTBC]Cu_2^{II} + DTBQ + 2H_2O \quad (2)$$

In the case of the complexes [Cu$_2$DABN-3Im$_4$]$^{4+}$ and [Cu$_3$DABN-3Im$_4$]$^{6+}$, it was impossible to determine the rate of the initial step, corresponding to stoichiometric oxidation of DTBC and reduction of the Cu(II) catalyst, because this reaction is either too fast or occurs with similar rate as step (2). The activity of the two complexes is similar (Table 1), indicating that coordination of DTBC in the ternary complex may occur to two Cu(A) centres, without involvement of the Cu(B) centre (Scheme 1). With the other complexes we were able to separate the two steps and determine the corresponding kinetic constants (Table 1).

While the rate of the first step always depends on the substrate concentration in a saturating fashion, the rate dependence of the second step on substrate concentration varies with the complex used. The complexes [Cu$_2$DABN-4Bz$_4$]$^{4+}$ and [Cu$_3$DABN-4Bz$_4$]$^{6+}$ exhibited substrate inhibition at high substrate concentrations, and therefore the kinetic parameters reported in Table 1 were estimated from the portion of the rate versus [substrate] plot in which inhibition could be neglected. As we observed in other cases [38], the inhibition effect often occurs when the ligand skeleton connecting the metal centres becomes too flexible, because in this case it is easier for the catechol to chelate each metal centre (Scheme 2), whereas a necessary condition for a fast two-electron transfer process is coordination of the catechol as a bridging ligand between the Cu(II) pair.

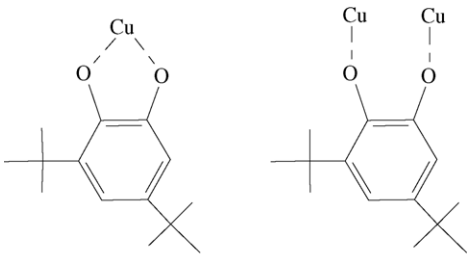

Scheme 2. Proposed structures for the binding of 3,5-di-*tert*-butylcatechol as a chelating ligand (structure I), and as a bridging ligand (structure II).

The different ligand architecture in the complexes derived from L-Lys-4Bz$_4$ has a positive effect on the activity, since they exhibit higher k_{cat} and k_{cat}/K_M values in both steps of DTBC oxidation than the series of binaphthyl complexes (Table 1). The dinuclear complex [Cu$_2$Lys-4Bz$_4$]$^{4+}$ is indeed the most active catalyst within the whole series, as shown by the value of turnover rate constant controlling the second, catalytic phase of the process. The high flexibility and reduced steric encumbrance of the lysine chain in these complexes, with respect to the binaphthyl residue in the DABN series, is clearly advantageous in the electron transfer steps involving intermediate formation of complexes with DTBC.

3.4. Catalytic oxidation of L-/D-Dopa derivatives

To assess the stereo-discriminating ability of the new Cu(II) complexes we carried out a comparative investigation of the catalytic oxidations of L- and D-Dopa and their methyl esters, L- and D-DopaOMe, as we did before with related dinuclear and trinuclear complexes [31,33,34]. Also in this case, the reagent MBTH was used as a trap for the unstable *o*-quinones, with which it forms covalent adducts. The copper complexes exhibited variable degree of stereoselectivity, but in all cases the preferred substrate had the L absolute configuration. This preference is probably dictated by the chirality of the binaphthyl or lysine residues, as shown by our previous studies on related complexes [31,33,34]. The kinetics of oxidation of Dopa derivatives showed monophasic behaviour, and it was therefore impossible to separate the two steps of the reaction. The plots of the rates of the catalytic reactions

Table 1
Kinetic parameters for the catalytic oxidation of 3,5-di-*tert*-butylcatechol in methanol-aqueous phosphate buffer, pH 5.0 at 20 °C

Complex	First step			Second step		
	K_M (mM)	k_{cat} (s^{-1})	k_{cat}/K_M ($M^{-1}\,s^{-1}$)	K_M (mM)	k_{cat} (s^{-1})	k_{cat}/K_M ($M^{-1}\,s^{-1}$)
[Cu$_2$DABN-3Im$_4$]$^{4+}$ [a]				0.09 ± 0.01	$(5.03 \pm 0.15) \times 10^{-3}$	58
[Cu$_3$DABN-3Im$_4$]$^{6+}$ [a]				0.10 ± 0.01	$(5.91 \pm 0.14) \times 10^{-3}$	58
[Cu$_2$DABN-4Bz$_4$]$^{4+}$	0.18 ± 0.02	$(1.56 \pm 0.04) \times 10^{-2}$	85	0.11 ± 0.02	$(9.37 \pm 0.63) \times 10^{-3}$	84
[Cu$_3$DABN-4Bz$_4$]$^{6+}$	0.08 ± 0.03	$(9.56 \pm 1.09) \times 10^{-3}$	120	0.04 ± 0.005	$(3.67 \pm 0.06) \times 10^{-3}$	105
[Cu$_2$Lys-4Bz$_4$]$^{4+}$	0.12 ± 0.01	$(6.11 \pm 0.09) \times 10^{-2}$	502	0.05 ± 0.01	$(2.58 \pm 0.05) \times 10^{-2}$	504
[Cu$_3$Lys-4Bz$_4$]$^{6+}$	0.10 ± 0.02	$(1.90 \pm 0.09) \times 10^{-2}$	183	0.10 ± 0.03	$(1.26 \pm 0.09) \times 10^{-2}$	127

[a] The catalytic reactions displayed monophasic behaviour.

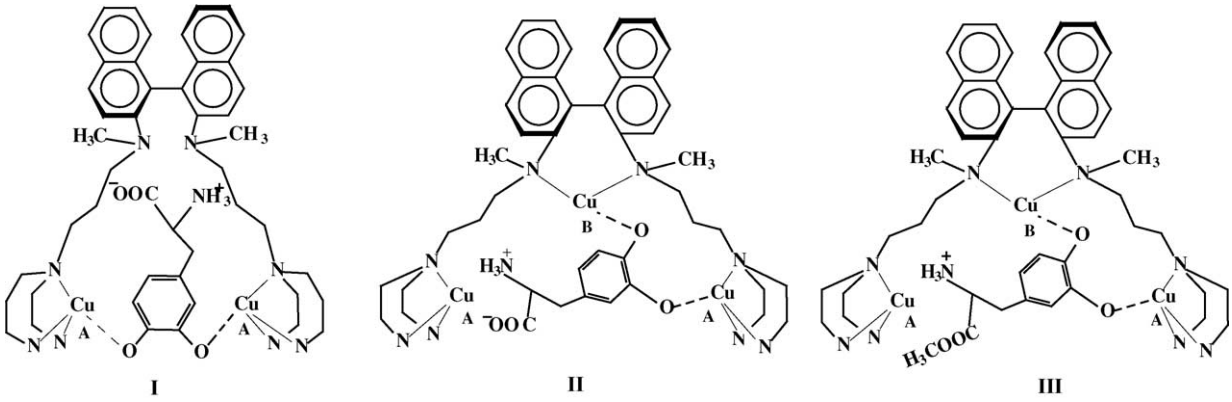

Scheme 3. Proposed structures for the putative intermediate adducts formed by the dinuclear (I) and trinuclear (II) copper complexes in the catalytic oxidation of L-, D-Dopa, and for the trinuclear copper complexes (III) in the catalytic oxidation of L-, D-DopaOMe.

as a function of the substrate concentration were hyperbolic in all cases. This enabled to determine the kinetic constants characterizing the catalytic process.

The dinuclear complex $[Cu_2DABN\text{-}3Im_4]^{4+}$ displays enantio-differentiating effects in the oxidation of L-, D-Dopa and L-, D-Dopa methyl esters, expressed in terms of *R*% index [34], that are in the same range as those previously reported for the related dinuclear complexes carrying benzimidazole instead of imidazole groups [31,34]. As discussed before, the chiral discrimination involves recognition between the binaphthyl residue and the chiral portion of the substrate [31,34]. This can be accounted for assuming that the productive catalyst–substrate interaction involves the binding of the catechol residue to the Cu(A) sites of the dinuclear complex leaving the amino acid portion of the molecule relatively free to approach the chiral binaphthyl residue (structure I in Scheme 3). In fact, the k_{cat} values, which reflect the efficiency of the electron transfer from the bound catechol residue to the coppers, are very similar for L- and D-Dopa derivatives, while the K_M values, which give an indication of the strength of the substrate binding interaction, show larger differences. The enantioselectivity is considerably larger for L-, D-Dopa methyl ester derivatives than for L-, D-Dopa, probably because in the latter case an electrostatic interaction between the negatively charged carboxylate group and the tertiary amine group(s) of the ligand prevents a closer approach to the binaphthyl residue. In the case of the trinuclear complex $[Cu_3DABN\text{-}3Im_4]^{6+}$, the catechol preferably binds to one Cu(A) site and the Cu(B) site (structure II in Scheme 3), because the two centres are bridged by hydroxo groups, while the amino acid portion of the substrate may interact at the Cu(A) site, keeping it far from the 1,1′-binaphthyl residue. With the L-, D-Dopa methyl ester substrates, the enantiodifferentiation is larger, probably because the interaction between the amino ester residue and the Cu(A) centre is weaker, allowing some interaction of this residue with the binaphthyl group. The alternative hypothesis of substrate binding as shown in structure III of Scheme 3, with a bridging catechol between two Cu(A) sites, would leave the ester group more free to approach the binaphthyl group, but is considered less likely because from our experience the Cu(A) and Cu(B) sites are kept in close proximity by bridging hydroxo groups in solution and should be a better target for catechol binding [34].

Both the complexes $[Cu_2DABN\text{-}4Bz_4]^{4+}$ and $[Cu_3DABN\text{-}4Bz_4]^{6+}$ show very little stereoselectivity towards L- and D-Dopa, even though they exhibit catalytic activity comparable to that of $DABN\text{-}3Im_4$ complexes (Table 2).

For the dinuclear complex, this behaviour can only be ascribed to the lengthening of the side chains connecting the side arms to the binaphthyl core, which apparently further facilitate strong immobilization of the carboxylate group of the substrate at the tertiary amine group(s) of the $DABN\text{-}4Bz_4$ ligand. With the L- and D-DopaOMe substrates, the stereoselectivity of oxidation is significant and approaches the value observed for $[Cu_2DABN\text{-}3Im_4]^{4+}$. This behaviour can be explained with arguments similar to those advanced above for $DABN\text{-}3Im_4$ complexes.

The catalytic behaviour of the complexes derived from L-Lys-$4Bz_4$ confirms that side chains of four carbon atoms between the chiral residue and the tridentate arms are not suitable to induce stereoselectivity in L-, D-Dopa oxidation. As observed for the 1,1′-binaphthyl complexes, enantiodifferentiation occurs in the oxidation of L-, D-Dopa methyl esters, but now the effect is limited to the dinuclear complex $[Cu_2Lys\text{-}4Bz_4]^{4+}$, while it is very reduced for the trinuclear complex $[Cu_3Lys\text{-}4Bz_4]^{6+}$ (Table 2). Clearly, the size of the chiral residue plays an important role in the chiral discrimination of substrates, but the data confirm that the large flexibility of the Lys-$4Bz_4$ ligand can have positive impact on the efficiency of the catalytic processes mediated by the corresponding Cu(II) complexes. As a matter of fact, the k_{cat}/K_M values for the oxidation of L-, D-Dopa methyl esters by $[Cu_2Lys\text{-}4Bz_4]^{4+}$ and $[Cu_3Lys\text{-}4Bz_4]^{6+}$ are the highest within the new series of copper catalysts.

Table 2
Kinetic parameters for the stereoselective catalytic oxidations of L- and D-Dopa and L- and D-DopaOMe in methanol-aqueous phosphate buffer, pH 8.5 at 20 °C

Substrate	K_M (mM)	k_{cat} (s^{-1})	k_{cat}/K_M	R%[a]
$[Cu_2DABN\text{-}3Im_4]^{4+}$				
L-Dopa	$(8.26 \pm 1.52) \times 10^{-2}$	$(5.86 \pm 0.30) \times 10^{-3}$	71	15
D-Dopa	$(1.02 \pm 0.18) \times 10^{-1}$	$(5.39 \pm 0.26) \times 10^{-3}$	52	
L-DopaOMe	$(2.32 \pm 0.55) \times 10^{-2}$	$(8.33 \pm 0.38) \times 10^{-3}$	360	59
D-DopaOMe	$(8.23 \pm 1.37) \times 10^{-2}$	$(7.51 \pm 0.34) \times 10^{-3}$	91	
$[Cu_3DABN\text{-}3Im_4]^{6+}$				
L-Dopa	$(8.61 \pm 0.72) \times 10^{-2}$	$(6.19 \pm 0.14) \times 10^{-3}$	72	4
D-Dopa	$(9.87 \pm 1.32) \times 10^{-2}$	$(6.65 \pm 0.32) \times 10^{-3}$	67	
L-DopaOMe	$(4.04 \pm 0.74) \times 10^{-2}$	$(1.06 \pm 0.04) \times 10^{-2}$	260	42
D-DopaOMe	$(7.27 \pm 0.39) \times 10^{-2}$	$(7.87 \pm 0.11) \times 10^{-3}$	108	
$[Cu_2DABN\text{-}4Bz_4]^{4+}$				
L-Dopa	$(4.12 \pm 0.70) \times 10^{-2}$	$(4.71 \pm 0.19) \times 10^{-3}$	114	4
D-Dopa	$(4.40 \pm 0.28) \times 10^{-2}$	$(4.68 \pm 0.74) \times 10^{-3}$	106	
L-DopaOMe	$(4.48 \pm 0.80) \times 10^{-2}$	$(9.62 \pm 0.41) \times 10^{-3}$	215	57
D-DopaOMe	$(1.26 \pm 0.16) \times 10^{-1}$	$(7.43 \pm 0.27) \times 10^{-3}$	59	
$[Cu_3DABN\text{-}4Bz_4]^{6+}$				
L-Dopa	$(5.76 \pm 0.60) \times 10^{-2}$	$(5.18 \pm 0.13) \times 10^{-3}$	90	4
D-Dopa	$(6.35 \pm 0.89) \times 10^{-2}$	$(5.30 \pm 0.29) \times 10^{-3}$	83	
L-DopaOMe	$(3.08 \pm 0.30) \times 10^{-2}$	$(1.31 \pm 0.27) \times 10^{-2}$	420	56
D-DopaOMe	$(8.43 \pm 0.64) \times 10^{-2}$	$(1.01 \pm 0.21) \times 10^{-2}$	120	
$[Cu_2Lys\text{-}4Bz_4]^{4+}$				
L-Dopa	$(1.21 \pm 0.11) \times 10^{-1}$	$(4.90 \pm 0.14) \times 10^{-3}$	40	5
D-Dopa	$(1.48 \pm 0.14) \times 10^{-1}$	$(5.29 \pm 0.17) \times 10^{-3}$	36	
L-DopaOMe	$(0.98 \pm 0.22) \times 10^{-2}$	$(2.07 \pm 0.18) \times 10^{-2}$	2120	40
D-DopaOMe	$(1.18 \pm 0.43) \times 10^{-2}$	$(1.07 \pm 0.11) \times 10^{-2}$	906	
$[Cu_3Lys\text{-}4Bz_4]^{6+}$				
L-Dopa	$(2.38 \pm 0.20) \times 10^{-1}$	$(8.36 \pm 0.28) \times 10^{-3}$	35	3
D-Dopa	$(2.60 \pm 0.17) \times 10^{-1}$	$(8.61 \pm 0.23) \times 10^{-3}$	33	
L-DopaOMe	$(0.84 \pm 0.12) \times 10^{-2}$	$(1.42 \pm 0.03) \times 10^{-2}$	1700	9
D-DopaOMe	$(0.76 \pm 0.13) \times 10^{-2}$	$(1.09 \pm 0.02) \times 10^{-2}$	1430	

[a] $R\% = [(k_{cat}/K_M)_L - (k_{cat}/K_M)_D]/[(k_{cat}/K_M)_L + (k_{cat}/K_M)] \times 100$ is taken as the index of enantioselectivity in the catalytic reactions.

4. Conclusion

We have synthesized three new chiral ligands and the corresponding dinuclear and trinuclear copper(II) complexes, which represent additional model systems for the active sites of Type 3 and Type 2–Type 3 copper proteins, respectively. The design of the ligands belonging to this family involves introduction of an optically active spacer ((*R*)-DABN, or L-Lys), ending with two tertiary amine donors, between chelating arms containing two tridentate nitrogen donors. Although the catalytic efficiency of the resulting complexes in the oxidation of catechols is lower than that exhibited by dinuclear complexes with hexadentate ligands containing a central xylyl spacer between analogous tridentate residues [27,28], the chiral complexes exhibit significant enantio-differentiating behaviour towards optically active substrates. The present investigation complements our previous reports on the stereoselective oxidations by the parent copper complexes of the DABN family [31,34], and enables to assess the effect of modulation of ligand design around the Cu(A) and Cu(B) sites. The results obtained here show that: (i) the length of the carbon chain connecting the chiral residue with the tridentate metal binding sites optimizes enantio-differentiation of the substrates by the complexes when the length of the carbon chain is of three atoms, (ii) the somewhat more lengthy synthetic procedure to replace the benzimidazole donors in the ligand with biologically more relevant imidazole donors does not produce significant improvement in the catalytic or stereoselective properties of the complexes, and (iii) the 1,1′-binaphthyl spacer has much stronger recognition power than the aliphatic lysine residue. Work is in progress to further elaborate on the ligand design to include into the carbon chains attached to the (*R*)-DABN or L-Lys spacers additional chiral centres, so that substrate recognition can occur closer to the metal sites involved in the catalytic event.

Acknowledgement

This work was supported by the Italian MIUR, through a PRIN project and a FIRST project. A.G. acknowledges CIRCMSB for financial support.

References

[1] L.I. Simandi (Ed.), Catalytic Activation of Dioxygen by Metal Complexes, Kluwer Academic, Dordrecht, 1992.

[2] E.I. Solomon, P. Chen, M. Metz, S.-K. Lee, A.E. Palmer, Angew. Chem. Int. Ed. 40 (2001) 4570–4590.
[3] E.A. Lewis, W.B. Tolman, Chem. Rev. 104 (2004) 1047–1076.
[4] A. Messerschmidt (Ed.), Multicopper Oxidases, World Scientific, Singapore, 1997.
[5] E.I. Solomon, U.M. Sundaram, T.E. Machonkin, Chem. Rev. 96 (1996) 2563–2605.
[6] K.D. Karlin, A.D. Zuberbuhler, in: J. Reedijk, E. Bouwman (Eds.), Bioinorganic Catalysis, Revised and Expanded, 2nd ed., Marcel Dekker, New York, 1999, pp. 469–534.
[7] M.E. Cuff, C. Miller, K.E. van Holde, W.A. Hendrickson, J. Mol. Biol. 278 (2000) 855–870.
[8] E.J. Land, C.A. Ramsden, P.A. Riley, Acc. Chem. Res. 36 (2003) 300–308.
[9] A. Sánchez-Ferrer, J.N. Rodrígez-López, F. García-Cánovas, F. García-Carmona, Biochim. Biophys. Acta 1247 (1995) 1–11.
[10] M. Tremolieres, J.B. Bieth, Phytochemistry 23 (1984) 501–505.
[11] C. Gerdeman, C. Eicken, B. Krebs, Acc. Chem. Res. 35 (2002) 183–191.
[12] A.L. Hughes, Immunogenetics 49 (1999) 106–114.
[13] T. Bertrand, C. Jolivalt, P. Briozzo, E. Caminade, N. Joly, C. Madzak, C. Mougin, Biochemistry 41 (2002) 7325–7333.
[14] A. Messerschmidt, R. Ladenstein, R. Huber, M. Bolognesi, L. Avigliano, R. Petruzzelli, A. Rossi, A. Finazzi-Agrò, J. Mol. Biol. 224 (1992) 179–205.
[15] V.N. Zaitsev, I. Zaitseva, M. Papiz, P.F. Lindley, J. Biol. Inorg. Chem. 4 (1999) 579–587.
[16] M.R. Malachowski, H.B. Huynh, L.J. Tomlinson, R.S. Kelly, J.W. Furbee Jr., J. Chem. Soc., Dalton Trans. (1995) 31–36.
[17] F. Zippel, F. Ahlers, R. Werner, W. Haase, H.-F. Nolting, B. Krebs, Inorg. Chem. 35 (1996) 3409–3419.
[18] R. Than, A.A. Feldman, B. Krebs, Coord. Chem. Rev. 182 (1999) 211–241.
[19] M.R. Malachowki, B. Dorsey, J.G. Sackett, R.S. Kelly, A.L. Ferko, R.N. Hardin, Inorg. Chim. Acta 249 (1996) 85–92.
[20] R. Wegner, M. Gottschaldt, H. Görls, E.-G. Jäger, D. Klemm, Chem. Eur. J. 7 (2001) 2143–2157.
[21] S.-C. Cheng, H.-H. Wei, Inorg. Chim. Acta 340 (2002) 105–113.
[22] K. Selmeczi, M. Réglier, M. Giorgi, G. Speier, Coord. Chem. Rev. 245 (2003) 191–201.
[23] C.-T. Yang, M. Vetrichelvan, X. Yang, B. Moubaraki, K.S. Murray, J.J. Vittal, Dalton Trans. (2004) 113–121.
[24] L. Casella, O. Carugo, M. Gullotti, S. Garofani, P. Zanello, Inorg. Chem. 32 (1993) 2056–2067.
[25] L. Casella, M. Gullotti, in: K.D. Karlin, Z. Tyeklar (Eds.), Bioinorganic Chemistry of Copper, Chapman and Hall, New York, 1993, pp. 292–305.
[26] L. Casella, E. Monzani, M. Gullotti, D. Cavagnino, G. Cerina, L. Santagostini, R. Ugo, Inorg. Chem. 35 (1996) 7516–7525.
[27] E. Monzani, L. Quinti, A. Perotti, L. Casella, M. Gullotti, L. Randaccio, S. Geremia, G. Nardin, P. Faleschini, G. Tabbì, Inorg. Chem. 37 (1998) 553–562.
[28] E. Monzani, G. Battaini, A. Perotti, L. Casella, M. Gullotti, L. Santagostini, G. Nardin, L. Randaccio, S. Geremia, P. Zanello, G. Opromolla, Inorg. Chem. 38 (1999) 5359–5369.
[29] E. Monzani, L. Casella, G. Zoppellaro, M. Gullotti, R. Pagliarin, R.P. Bonomo, G. Tabbì, G. Nardin, L. Randaccio, Inorg. Chim. Acta 282 (1998) 180–192.
[30] L. Santagostini, M. Gullotti, R. Pagliarin, E. Bianchi, L. Casella, E. Monzani, Tetrahedron: Asymmetry 10 (1999) 281–295.
[31] M.C. Mimmi, M. Gullotti, L. Santagostini, A. Saladino, L. Casella, E. Monzani, R. Pagliarin, J. Mol. Catal. A: Chem. 204–205 (2003) 381–389.
[32] M.C. Mimmi, M. Gullotti, L. Santagostini, R. Pagliarin, L. De Gioia, E. Monzani, L. Casella, Eur. J. Inorg. Chem. (2003) 3934–3944.
[33] L. Santagostini, M. Gullotti, R. Pagliarin, E. Monzani, L. Casella, Chem. Commun. (2003) 2186–2187.
[34] M.C. Mimmi, M. Gullotti, L. Santagostini, G. Battaini, E. Monzani, R. Pagliarin, G. Zoppellaro, L. Casella, Dalton Trans. (2004) 2192–2201.
[35] N. Wei, N.N. Murthy, Z. Tyeklàr, K.D. Karlin, Inorg. Chem. 33 (1994) 1177–1183.
[36] L. Casella, O. Carugo, M. Gullotti, S. Doldi, M. Frassoni, Inorg. Chem. 35 (1996) 1101–1113.
[37] L. Di Bari, G. Pescitelli, P. Salvadori, J. Am. Chem. Soc. 121 (1999) 7998–8004.
[38] G. Battaini, E. Monzani, L. Casella, L. Santagostini, R. Pagliarin, J. Biol. Inorg. Chem. 5 (2000) 262–268.
[39] A. Granata, E. Monzani, L. Casella, J. Biol. Inorg. Chem. 9 (2004) 903–913.